Advances in Aircraft and Spacecraft Science, *Vol. 4, No. 5 (2017) 585-611*
DOI: https://doi.org/10.12989/aas.2017.4.5.585

Stochastic thermo-mechanically induced post buckling response of elastically supported nanotube-reinforced composite beam

Virendra Kumar Chaudhari[1a], Niranjan L. Shegokar[2a] and Achchhe Lal[*3]

[1]D C National polytechnic, Siddhartha Nagar, U.P 272153, India
[2]D Y Patil Institute of Engineering & Technology, Pune, India
[3]S.V. National Institute of Technology, Surat-395007, India

(Received Ocotber 27, 2016, Revised June 11, 2017, Accepted June 12, 2017)

Abstract. This article covenants with the post buckling witticism of carbon nanotube reinforced composite (CNTRC) beam supported with an elastic foundation in thermal atmospheres with arbitrary assumed random system properties. The arbitrary assumed random system properties are be modeled as uncorrelated Gaussian random input variables. Unvaryingly distributed (UD) and functionally graded (FG) distributions of the carbon nanotube are deliberated. The material belongings of CNTRC beam are presumed to be graded in the beam depth way and appraised through a micromechanical exemplary. The basic equations of a CNTRC beam are imitative constructed on a higher order shear deformation beam (HSDT) theory with von-Karman type nonlinearity. The beam is supported by two parameters Pasternak elastic foundation with Winkler cubic nonlinearity. The thermal dominance is involved in the material properties of CNTRC beam is foreseen to be temperature dependent (TD). The first and second order perturbation method (SOPT) and Monte Carlo sampling (MCS) by way of CO nonlinear finite element method (FEM) through direct iterative way are offered to observe the mean, coefficient of variation (COV) and probability distribution function (PDF) of critical post buckling load. Archetypal outcomes are presented for the volume fraction of CNTRC, slenderness ratios, boundary conditions, underpinning parameters, amplitude ratios, temperature reliant and sovereign random material properties with arbitrary system properties. The present defined tactic is corroborated with the results available in the literature and by employing MCS.

Keywords: CNTRC beam; post buckling load; second order perturbation technique; Monte Carlo simulation; elastic foundation; arbitrary system properties

1. Introduction

The carbon nanotubes (CNT) are being progressively rummage-sale in wind turbines, tissue engineering, thin films of shape memory alloys, nano-electromechanical systems, micro sensors, micro actuators, telecommunications and transport industry. CNTRC have marvelous mechanical, electrical and thermal properties by varying the spreading and composition of CNT. CNTRC have

∗Corresponding author, Ph.D., E-mail: achchhelal@med.svnit.ac.in
[a]Ph.D.

http://www.techno-press.org/?journal=aas&subpage=7 ISSN: 2287-528X (Print), 2287-5271 (Online)

become eye-catching structural materials not only in the weight-sensitive aerospace industry but also in the marine, armor, automobile, railway and sport goods diligences.

The beam is frequently supported by various elastic foundations. The beam supported by the elastic foundation are being increasingly used in operational activities of large transportation aircraft on runways, launching pad of missiles and tops, suspension systems in automobiles, ship and bridge structures etc.

A beam is one of the very essential long slender structural members generally subjected to in-plane loadings that produce significant buckling effects. This buckling effect is measured by proving in-plane axial load and this in-plane load in terms as buckling load. Hence, for optimum stability of beam, the evaluation of buckling load under the action of in-plane loadings is essential.

The buckling load may be classified as linear and post buckling load by providing external amplitude in the nonlinear stiffness matrix. The study of the postbuckling load response of the structure is extremely important for structural components to prevent botches and optimum design. Thus, this topic has been fascinating many researchers for several years. The modeling and determination of the elastic foundation to obtain the accurate response of the overall structure are also a matter of concern in the practice. To represent the accurate behavior of practical underpinning two parameters Pasternak with Winkler cubic nonlinearity has proved to be most useful and very useful for design perspective.

The system properties of CNTRC beam can become tentative due to changes in various manufacturing conditions such as material gradations, curing temperature, pressure and precise measurement of micro level mechanical properties. Due to imprecise measurement of above parameters, significant uncertainties in their material and geometrical properties may be raised. For the safe and reliable design of CNTRC structure, these uncertainties should be quantified probabilistically so that error between actual and forecasted response should be least.

The uncertainties in underpinning stiffness are also inherent in nature. The sympathetic of the influence of the qualms in thermomechanical properties and underpinning parameters on the post buckling loads concluded statistical model grounded on either perturbation approach or sampling approach is extremely important for a reliable and safe design of such structures.

Much assessment has been accomplished on the determination of carbon nanotube reinforced composite mechanical properties in contemporary years. The CNT are used as significant reinforcement materials for high performance structural composites with substantial application potentials discussed by Thostenson et al. (2001), Esawi and Farag (2007), Salvetat and Rubio (2002). Academics probed the mechanical properties of CNTRC by experimentally, analytically and statistically. Thermal properties of single walled carbon nanotube (SWCNT) composite thick films were explored by Bonnet et al. (2007). Song and Youn (2006) detected that the blender of 7% SWCNT into the polymer matrix boosts the thermal conductivity of the composite by 55% while the electrical conductivity increases by numerous orders of extent. The operative pliant properties of the nanocomposites filled with CNT investigated by the asymptotic expansion homogenization (AEH) method, micromechanics performances and Mori–Tanaka way by Seidel and Lagoudas (2006).

Han and Elliott (2007) assessed the axial and transverse elastic moduli of carbon nanotube composites with different volume fractions of CNT through constant-strain energy minimization scheme using molecular dynamics. Meguid and Sun (2004) probed the tensile and shear strength of CNTRC interfaces by single shear-lap analysis. Wan et al. (2005) explored the effective modulus of the CNT reinforced polymer composite assimilation of CNT in the polymer composite, CNT can lead to noteworthy improvements in the composite properties at very low volume fractions. Wuite and Adali (2005) evaluated that the stiffness of CNTRC beams can be upgraded meaningfully of a small percentage of CNTs by homogeneous dispersion.

Certain exertion has been addressed in the past by researchers for evaluation of initial and post buckling load of CNTRC beam via deterministic approach. Shen (1995) assessed for a biaxially compressed simply supported moderately thick rectangular plate resting on a two-parameter (Pasternak-type) elastic foundation by Reissner-Mindlin plate theory. Das and Singh (2012) assessed post-buckling riposte of laminated composite plates using higher order shear deformation theory associated with Green–Lagrange type nonlinearity. Vodenitcharova and Zhang (2006) established a continuum mechanics model. They discovered the bending and buckling of a nanocomposite beam. Shen and Zhang (2010) considered post buckling behavior of functionally graded CNTRC plates subjected to in-plane temperature loading via micromechanical archetypal and multi-scale tactic.

Pradhan and Reddy (2011) reconnoitered the thermo-mechanical buckling behaviour of SWCNT on Winkler foundation applying non-local elasticity theory and differential transformation method. Yas and Samadhi (2012) examined the natural frequency and critical buckling load of CNTRC beams with or without an elastic foundation for various boundary conditions via differential quadrature mode concluded Hamilton's principle. Wattanasakulpong and Ungbhakorn (2013) premeditated the structural behaviors of elastically supported CNTRC beams containing shear strain effect via the rule of mixture. Hosseiniara et al. (2012) reconnoiter the buckling behavior of short clamped CNT Timoshenko beam. Malekzadeh and Shojaee (2013) premeditated the buckling behavior of laminated CNTRC plates via the first-order shear deformation theory (FSDT). Rafiee et al. (2013) premeditated the buckling behavior of piezoelectric surface bonded layers CNTRC beams with von Karman type geometric nonlinearity. Shen and Xiang (2013) deliberated the structural behaviors of CNTRC beams resting on an elastic foundation in thermal environments using HSDT with semi analytical approach.

It has been practiced in the engineering fields to analyze the strctural response by assuming system properties as determinant. However, in actual condition, these random system properties are not deterministic. For higher safely and reliability required for sensitive applications, the system parameters are assumed as probabilistic which gives mean response and the variation in the randomness of system parameters. However, such assumptions are rarely encountered in engineering reality and need to address uncertainties in the design for sensitive applications for an ideal situation. The study related to post buckling analyses of CNTRC beam; plate and panels using stochastic analysis are very limited.

In this direction, Hisada and Nakagiri (1980) presented a methodology of SFEM applied to uncertain eigenvalue problem of linear vibration, which arises from the fluctuation of the overall stiffness due to uncertainty. Mean centered perturbation technique has been employed to handle the random behavior. Vanmarcke and Grigoriu (1983) also used the stochastic finite element method to demonstrate the use of spatial averaging of random fields to simple beams with random rigidity. Kaminski (2001) presented the second order perturbation probabilistic method for stress based finite element method (FEM). Kaminski introduced the second order variational equation of the complementary energy principle. Stefanou (2009) surveyed the past and recent developments in finite element method in computational stochastic mechanics. Elishakoff et al. (1996) developed a governing equation of mean and covariance for a beam with stochastically varying stiffness under deterministic loading. Klieber and Hien (1992) presented stochastic finite element method (SFEM) based on perturbation technique using Taylor series expansion of the governing equations to evaluate the expectation and covariance of the structural response by random input variables.

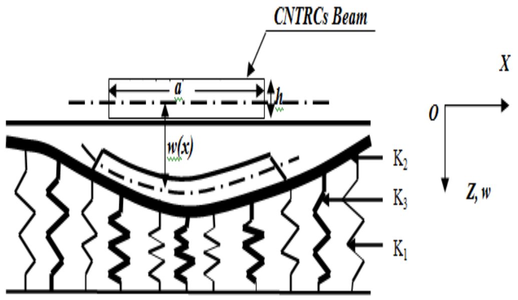

Fig. 1 Geometry of CNTRC beam resting on nonlinear elastic foundation

Locke (1993) presented structural response of plates using iterative techniques and method of linearization in the thermal environment. Chang and Chang (1994) studied the non-deterministic dynamic responses of a nonuniform beam in combination with MCS and perturbation technique using FEM. Singh and Grover (2013) offered the various stochastic approaches and their applicability to quantify various uncertainties in composite structures. Yang *et al*. (2005) reconnoitered the buckling and bending characteristics FGM plates based on Reddy's HSDT plate theory and a semi-analytical method with system randomness of low variability. Lal et al. (2012) and Lal *et al*. (2013) reconnoitered the outcome of random system properties on initial and post buckling of functionally graded plates stayed with and without to thermal environment using HSDT based C^0 linear and nonlinear FEM united with and without direct iterative method in combination with FOPT. Shegokar and Lal (2013) deliberate the post buckling reaction of the piezoelectric bonded FGM beam subjected to thermoelectromechanical loadings using HSDT with von-Karman nonlinearity in the non-deterministic framework.

The contribution of this paper is to provide a probabilistic tool for handling micromechanical and geometrical properties and their effect on post buckling reaction of elastically supported CNTRC beam by assuming random system properties. The non-deterministic framework analysis based on FOPT, SOPT, and MCS in combination with C^0 nonlinear FEM through HSDT with von-Karman nonlinearity via direct iterative procedure is used to evaluate the statistics of buckling load.

2.Mathematical formulation

2.1 Geometric configuration

Consider a CNTRC beam supported by nonlinear elastic foundation consist of linear and nonlinear spring and shear foundation of length *a* and thickness *h* located in one dimensional plane with its coordinate definition and material directions of typical lamina in (x, z) coordinate system as shown in Fig. 1. The CNTRC beam is assumed to be attached to the foundation excluding any separation takes place in the process of deformation. The interaction between the beam and the supporting foundation follows the two parameters model (Pasternak-type) with Winkler cubic nonlinearity as Shegokar and Lal (2013).

$$p = K_1 w + K_2 w^3 + K_3 \nabla w \tag{1}$$

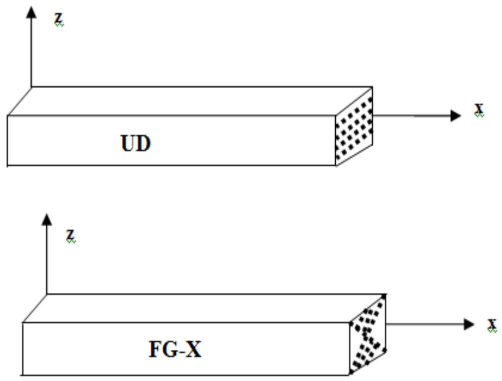

Fig. 2 Configurations of the CNTRC in composite beams

where p and w are the foundation reaction per unit area and transverse displacement, respectively, The parameters ∇, K_1, K_2, and K_3 are Laplace differential operator, linear normal, shear and nonlinear normal stiffnesses of the foundation, respectively. This model is simply known as Winkler type when the shear stiffness of the foundation is neglected.

2.2 Material properties of CNTRC beams

The uniform distribution (UD) and functionally graded FG-X shape distribution of carbon nanotubes in the depth direction of the composite beams (z axis direction) are deliberated and shown in Fig. 2. The Density of CNT within the area is constant and the volume fraction varies through the depth of the beam. In the present investigation, an embedded carbon nanotube in a polymer matrix is used. Thus there is no unforeseen interface between the CNT and polymer matrix in the entire region of the beam. It is presumed that the CNTRC beams are made of a mixture of SWCNTs and an isotropic matrix. To appraise the operative material properties of CNTRC, the rule of the mixture based on the Mori-Tanaka model (2, 6, and 21) micromechanical tactic is employed. According to rule of mixture model, the operative Young's moduli and shear modulus of CNTRC beams can be articulated as

$$E_{11} = \eta_1 V_{cn} E_{11}^{cn} + V_m E^m \tag{2}$$

$$\frac{\eta_2}{E_{22}} = \frac{V_{cn}}{E_{22}^{cn}} + \frac{V_m}{E^m} \tag{3}$$

$$\frac{\eta_3}{G_{12}} = \frac{V_{cn}}{G_{12}^{cn}} + \frac{V_m}{E^m} \tag{4}$$

where E_{11}^{cn}, E_{12}^{cn}, G_{12}^{cn}, E_{m} and G_{m} are Young's moduli and shear modulus of the SWCNTs and matrix, respectively are the equivalent properties for the matrix for isotropic materials. η_j (j=1, 2, 3) are the CNT efficiency parameters to cogitate the size dependent material properties.

In addition, V_{cn} and V_m are the volume fraction of the CNT and the matrix which satisfy the correlation of $V_{cn}+V_m=1$.

Similarly, Poisson's ratio v and mass density ρ of the CNTRC beams can be articulated as

$$\nu = V_{cn}\nu^{cn} + V_m\nu^m \quad \rho = V_{cn}\rho^{cn} + V_m\rho^m \tag{5}$$

Where v^{cn}, v^m, ρ^{cn}, and ρ^m are the Possion's ratios and densities of CNT and matrix, respectively.

The different distributions of the carbon nanotubes along the depth direction of the CNTRC beam depicted in Fig. 1 is assumed to be as follows:

UD case

$$V_{cn} = V_{cn}^* \tag{6}$$

FG-Λ case

$$V_{cn} = 2\left(1 + \frac{2z}{h}\right)V_{cn}^* \tag{7}$$

FG-X case

$$V_{cn} = 2 - 4\frac{|z|}{h}V_{cn}^* \tag{8}$$

where V_{cn}^* is the volume fraction of CNTs and can be evaluated as

$$V_{cn} = \frac{W_{cn}}{W_{cn} + \left(\frac{\rho^{cn}}{\rho^m}\right) - \left(\frac{\rho^{cn}}{\rho^m}\right)W_{cn}} \tag{9}$$

Correspondingly, the effective thermal expansion coefficients in the longitudinal and transverse directions (α_{11}, α_{22}) graded in the z direction can be expressed by the Shapery (1968)

$$\alpha_{11} = \frac{V_{cn}E_{11}^{cn}\alpha_{11}^{cn} + V_m E^m \alpha^m}{V_{cn}E_{11}^{cn} + V_m E^m} \tag{10}$$

$$\alpha_{22} = \left(1 + \nu_{12}^{cn}\right)V_{cn}\alpha_{22}^{cn} + \left(1 + \nu^m\right)V_m\alpha^m - \nu_{12}\alpha_{11} \tag{11}$$

It is presumed that the material properties of CNT and matrix are the functions of temperature, so that the operative material properties of CNTRC beam, like Young's modulus, shear modulus, and thermal expansion coefficients, are also functions of temperature T and position z.

2.3 Displacement field model

For an arbitrary CNTRC beam, the components of displacement field model can be express as the modified displacement field components along x and z directions of an arbitrary point within the beam based on the HSDT using C^0 continuity can be expressed as Shegokar and Lal (2013)

$$\bar{u}(x,z) = u + f_1(z)\psi_x + f_2(z)\phi_x; \quad \bar{w}(x,z) = w \tag{12}$$

Where u, w, Ψ_x and $\phi = \frac{\partial w}{\partial x}$ are the mid-plane axial displacement, transverse displacement, rotation of normal to the mid-plane along y- axis and slope along x- axis, respectively.

The parameter $f_1(z)$ and $f_2(z)$ are expressed as

$$f_1(z) = C_1 z - C_2 z^3, \quad f_2(z) = -C_4 z^3, \quad \text{With } C_1 = 1,\ C_2 = C_4 = 4/3h^2 \tag{13}$$

The displacement vector for the modified C^0 continuous model can be written as

$$\{q\} = [u \quad w \quad \theta_x \quad \psi_x]^T \tag{14}$$

2.4 Strain displacement relation

The aggregate strain vector containing linear strain (in forms of mid plane deformation, rotation of normal and higher order terms), non-linear strain (von-Karman type), thermal strains vectors acquaintance with the displacement for CNTRC beam can be articulated as

$$\{\bar{\varepsilon}\} = \{\bar{\varepsilon}^L\} + \{\bar{\varepsilon}^{NL}\} - \{\bar{\varepsilon}^T\} \tag{15}$$

Where $\{\bar{\varepsilon}^L\}$, $\{\bar{\varepsilon}^{NL}\}$ and $\{\bar{\varepsilon}^T\}$ are the linear, non-linear and thermal strain vectors, correspondingly.

From Eq. (15), the linear strain tensor using HSDT can be written as

$$\bar{\varepsilon}^L = [B]\{q\} \tag{16}$$

where $[B]$ and $\{q\}$ are the geometrical matrix and displacement field vector, correspondingly.

The nonlinear strain vector $\{\bar{\varepsilon}^{NL}\}$ can be written as

$$\bar{\varepsilon}^{NL} = \frac{1}{2}[A_{nl}]\{\phi_{nl}\}$$

Where

$$\{A_{nl}\} = \frac{1}{2}\left[\frac{\partial w}{\partial x}\right]^T \text{ and } \{\phi_{nl}\} = \left\{\frac{\partial w}{\partial x}\right\} \tag{17}$$

The thermal strain vector $\{\bar{\varepsilon}^T\}$ induced by uniform and non-uniform temperature change can be articulated as

$$\{\bar{\varepsilon}^T\} = \{\alpha_x\}\Delta T \tag{18}$$

Where $\{\alpha_x\}$ is coefficients of thermal expansion along the x direction, and ΔT is the change in temperature in the CNTRC beam considered as uniform and non-uniform type.

The unvarying change in temperature (ΔT) can be articulated as

$$\Delta T = T - T_0 \tag{19}$$

Where T and T_0 are the unvarying temperature rise and room temperature, respectively. For the present case, the room temperature is assumed as 300 K.

2.5 Stress-strain relation

The relation between stress $\{\bar{\sigma}\}$ and strain for the plane-stress case using thermo-elastic constitutive relation can be written as

$$\{\bar{\sigma}\} = [Q]\{\bar{\varepsilon}\} \quad (20)$$

$$\begin{Bmatrix} \bar{\sigma}_x \\ \bar{\tau}_{xz} \end{Bmatrix} = \begin{bmatrix} Q_{11} & 0 \\ 0 & Q_{55} \end{bmatrix} \left\{ \{\bar{\varepsilon}^L\} + \{\bar{\varepsilon}^{NL}\} - \{\bar{\varepsilon}^T\} \right\} \quad (21)$$

Where

$$Q_{11}(z) = \frac{E_z}{1-\nu^2(z)}, \quad Q_{55}(z) = G_{12}(z) \quad (22)$$

2.6 Strain energy of CNTRC beam

The strain energy (Π_1) of the CNTRC beam undergoing large deformation can be expressed as

$$\Pi_1 = U_L + U_{NL} \quad (23)$$

The linear stain energy (U_L) of the CNTRC beam is given by

$$U_L = \int_A \frac{1}{2}\{\bar{\varepsilon}^L\}^T [Q]\{\bar{\varepsilon}^L\} dA = \int_A \frac{1}{2}\{\bar{\varepsilon}^L\}^T [D]\{\bar{\varepsilon}^L\} dA \quad (24)$$

where [D] and $\{\bar{\varepsilon}^L\}$ are the elastic stiffness matrix and linear strain vector respectively.

The nonlinear strain energy (U_{NL}) of the CNTRC beam can be rewritten as

$$U_{NL} = \int_A \frac{1}{2}\{\bar{\varepsilon}^L\}[D_1]\{\bar{\varepsilon}^{NL}\}^T dA + \frac{1}{2}\int_A \{\bar{\varepsilon}^{NL}\}[D_2]\{\bar{\varepsilon}^L\}^T dA + \frac{1}{2}\int_A \{\bar{\varepsilon}^{NL}\}[D_3]\{\bar{\varepsilon}^{NL}\}^T dA \quad (25)$$

Where D_1, D_2, and D_3 are the elastic stiffness matrices of the CNTRC beam, respectively.

2.7 Strain energy due to foundation

The strain energy due to elastic foundation having shear deformable layer with Winkler cubic nonlinearity is expressed as

$$U_F = \frac{1}{2}\int_v pw dV \quad (26)$$

The strain energy due to the foundation is expressed as

$$U_F = \frac{1}{2}\int_A \left\{ K_1 w^2 + \frac{1}{2} K_3 w^4 + K_2 \left[(w,_x)^2 + (w,_x)^2 \right] \right\} dA \quad (27)$$

$$U_F = \frac{1}{2}\int_A \begin{Bmatrix} w \\ w,_x \end{Bmatrix}^T \begin{bmatrix} K_1 & 0 \\ 0 & K_2 \end{bmatrix} \begin{Bmatrix} w \\ w,_x \end{Bmatrix} dA + \frac{1}{2}\int_A \begin{Bmatrix} w \\ w,_x \end{Bmatrix}^T \begin{bmatrix} K_3 w^2 & 0 \\ 0 & 0 \end{bmatrix} \begin{Bmatrix} w \\ w,_x \end{Bmatrix} dA \quad (28)$$

2.8 Work done due to thermal loadings

The potential of work (Π_2) storage due to thermal loadings can be written as

$$\Pi_2 = \frac{1}{2}\int_A N_0^T \left(w,_x\right)^2 dA \tag{29}$$

The thermal compressive stress/unit length N_0^T can be expressed as

$$N_0^T = \left[N_x^T \quad M_x^T \quad P_x^T \right] \tag{30}$$

The Eq. (30) can be further written as

$$N_0^T = \int_{-h/2}^{h/2} (1, z, z^3)(Q_{11})\ \alpha \Delta T dz \tag{31}$$

3. Finite element model

The present study includes a C^0 one-dimensional Hermitian beam element having 4 DOFs each node. Shegokar and Lal (2013) expressed as this type of beam element geometry and the displacement vector.

$$\{q\} = \sum_{i=1}^{NN} N_i \{q\}_i ; \qquad x = \sum_{i=1}^{NN} N_i x_i ; \tag{32}$$

N_i and $\{q\}_i$ signify the interpolation function for the *i*th node and the vector of unknown displacements for the *i*th node, correspondingly. The parameter *NN* shows the number of nodes per element and x_i shows the Cartesian coordinate. The axial displacement and rotation of normal are represented by linear interpolation function and while, for transverse displacement and slope by Hermite cubic interpolation functions.

Using finite element model Eq. (32), Eq. (23) can be expressed a

$$\Pi_1 = \sum_{e=1}^{NE} \Pi_a^{(e)} = \sum_{e=1}^{NE} \left(U_L^{(e)} + U_{NL}^{(e)} \right) \tag{33}$$

Where, *NE* and (e) denote the number of elements and elemental, respectively.

Substituting Eq. (24) and Eq. (25) into Eq. (33) and can be further expressed as

$$\Pi_1 = \frac{1}{2}\sum_{e=1}^{NE}\left[\{q\}^{T(e)} \left[K_l + K_{nl}\right]^{(e)} \{q\}^{(e)} \right] = \{q\}^T \left[K_l + K_{nl} \right] \{q\} \tag{34}$$

Here $\left[K_{nl}\right] = \frac{1}{2}\left[K_{nl_1}\right] + \left[K_{nl_2}\right] + \frac{1}{2}\left[K_{nl_3}\right]$

Where, $[K_l]$, $[K_{nl1}]$, $[K_{nl2}]$, $[K_{nl3}]$ and $\{q\}$ are defined as global linear, nonlinear stiffness matrices and global displacement vector, respectively.

Similarly, using finite element model Eq. (32), Eq. (28) after assembly procedure can be written

$$\Pi_F = \sum_{e=1}^{NE}\left(\Pi_F^{(e)}\right) = \left\{\Delta^{(e)}\right\}\left[K_{fl} + K_{fnl}\left(\Delta\right)\right]^{(e)}\left\{\Delta^{(e)}\right\} = \{q\}\left[K_{fl} + K_{fnl}\left(q\right)\right]\{q\} \tag{35}$$

Where, $[K_{fl}]$ and $[K_{fnl}(q)]$ is the global linear and nonlinear foundation stiffness matrices, respectively.

Using finite element model Eq. (32), Eq. (29) after summing over the entire element can be written as

$$\Pi_2 = \sum_{e=1}^{NE}\Pi_2^{(e)} = \frac{1}{2}\sum_{e=1}^{NE}\{q\}^{T(e)}\lambda\left[K_g\right]^{(e)}\{q\}^{(e)} = \frac{1}{2}\lambda\{q\}^T\left[K_g\right]\{q\} \tag{36}$$

where, λ and $[K_{(G)}]$ are defined as the thermal buckling load parameters and the global geometric stiffness matrix, respectively.

4. Governing equation

The governing equation of thermo-mechanically induced post buckling load of CNTRC beam is obtained by the variational principal of generalization. For the post buckling analysis, the minimization of the first variation of total potential energy Π (Π_1+Π_f-Π_2) with respect to generalized displacement vector is given by

$$\frac{\partial}{\partial\{q\}}\left(\Pi_1 + \Pi_f - \Pi_2\right) = 0 \tag{37}$$

By Substituting Eqs. (34)-(36) into Eq. (37), the standard eigenvalue problem can be expressed as

$$\{[K_L + K_{NL}] + \lambda[\mathrm{K}_G]\}\{\mathrm{q}\} = 0 \tag{38}$$

$$[K]\{q\} = \lambda[K_g]\{q\} \tag{38a}$$

where

$$[K] = \{[K_l] + [K_{nl}] + [K_{lf}] + [K_{nlf}] - [K_g]\} \tag{38b}$$

The Eq. (38) is the nonlinear post buckling equation. In the deterministic environment, the Eq. (38) is evaluated and solved by assuming as eigenvalue problem using direct iterative methods, incremental methods etc. However, in random environment, Eq. (38) cannot be solved using above mentioned approaches. For this purpose, the direct iterative method is successfully combined with mean cantered SOPT, and MCS to obtain the solution of the random nonlinear governing equations. Further analysis is required which is explained in subsection 5.2.

5. Solution approach

5.1 A direct iterative method for post buckling problem

The nonlinear eigenvalue problem as given in Eq. (38) is solved using the direct iterative procedure by assuming that the random changes in eigenvector during iterations does not affect much the nonlinear stiffness matrix (Shegokar and Lal 2013) and solved by implementing probabilistic approaches as given below.

5.2 Stochastic perturbation approach

In the present non-deterministic analysis, finite element based on FOPT, SOPT and MCS methods are adopted to quantify the structural response uncertainties by doing an explicit treatment of uncertainties in any or combined quantities. The existing uncertain variations in parameters may have significant effects on the fundamental structural characteristic in the form of post buckling load; consequently, this uncertain parameter must affect the final design.

The FOPT and SOPT based on Taylor series expansion are used to formulate the linear relationship between some characteristics of the random response and random structural constraints on the basis of perturbation tactic. However, the applicability of these methods is limited due to valid for the small coefficient of variation (COV) of input random variables Shegokar and Lal (2013). The descriptions of these methods are given as follows.

In this method, the stiffness matrix *K*, the mass matrix *M* and displacement vector *q*; are expended in terms of the random variable α_i which represent the structural uncertainty existing in the CNTRC elastically supported beam, as follows

$$\begin{aligned}
[K] &= \left[K^{(0)}\right] + \sum_{i=1}^{N}\left[K_i^{(1)}\right]\alpha_i + \frac{1}{2}\sum_{i=1}^{N}\sum_{j=1}^{N}\left[K_{ij}^{(2)}\right]\alpha_i\alpha_j \\
.[q] &= \left[q^{(0)}\right] + \sum_{i=1}^{N}\left[q_i^{(1)}\right]\alpha_i + \frac{1}{2}\sum_{i=1}^{N}\sum_{j=1}^{N}\left[q_{ij}^{(2)}\right]\alpha_i\alpha_j \\
[\lambda] &= \left[\lambda^{(0)}\right] + \sum_{i=1}^{N}\left[\lambda_i^{(1)}\right]\alpha_i + \frac{1}{2}\sum_{i=1}^{N}\sum_{j=1}^{N}\left[\lambda_{ij}^{(2)}\right]\alpha_i\alpha_j \\
\left[K_g\right] &= \left[K_g^{(0)}\right] + \sum_{i=1}^{N}\left[K_{gi}^{(1)}\right]\alpha_i + \frac{1}{2}\sum_{i=1}^{N}\sum_{j=1}^{N}\left[K_{gij}^{(2)}\right]\alpha_i\alpha_j
\end{aligned} \tag{39}$$

where $K^{(0)}$, $q^{(0)}$, $\lambda^{(0)}$ and K_g^0 are the mean value of response variables $K_i^{(1)}$ and $K_i^{(2)}$ is the first and second order derivatives evaluated at the mean value, α_o, which can be expressed as following zeroth, first and second order terms are obtained as:

Zeroth order perturbation equation

$$\left(\left(K^{(0)}\right) - \lambda^{(0)}\left[K_{g0}\right]\right)\left\{q^{(0)}\right\} = 0 \tag{40}$$

First order perturbation equation

$$\left(\left(K^{(0)}\right) - \lambda^{(0)}\left[K_{g0}\right]\right)\left\{q_i^{(1)}\right\} + \left(\left[K_i^1\right] - \lambda^{(0)}\left[K_{gi}^1\right] - \lambda_i^{(1)}\left[K_{g0}\right]\right)\times\left\{q^{(0)}\right\} = 0 \tag{41}$$

Second order perturbation equation

$$\begin{aligned}
&\left(\left[K_i^1\right] - \lambda^{(0)}\left[K_{gi}^1\right] - \lambda_i^{(1)}\left[K_{g0}\right]\right)\left\{q_i^{(1)}\right\} + \frac{1}{2}\left(\left(K^{(0)}\right) - \lambda^{(0)}\left[K_{g0}\right]\right)\left\{q_{ij}^{(2)}\right\} \\
&+ \frac{1}{2}\left(\left[K_{ij}^2\right] - \lambda^{(0)}\left[K_{gij}^2\right] - \lambda_{ij}^{(2)}\left[K_{g0}\right]\right)\times\left\{q^{(0)}\right\} = 0
\end{aligned} \tag{42}$$

Zeroth order Eq. (40) is the deterministic equation which can be solved by conventional eigen solution procedure. First order and second order Eqs. (41) and (42) represent its random counterparts which can be solved using probabilistic approach Shegokar and Lal (2013).

From these mean and covariance matrix of response vector, $\{\lambda\}$ can be obtained as

$$\langle\{\lambda\}\rangle \approx \{\lambda_0\} + \frac{1}{2}\sum_{i=1}^{N}\sum_{j=1}^{N}\{\lambda_{ij}{}^{II}\}Cov\left[\alpha_i,\alpha_j\right] \tag{43}$$

$$Cov\left[\{\lambda\},\{\lambda\}\right] \approx \sum_{i=1}^{N}\sum_{j=1}^{N}\{\lambda_i^{(1)}\}\left(\{\lambda_j^{(1)}\}\right)^T Cov\left[\alpha_i,\alpha_j\right] \tag{44}$$

Eq. (44) can be written a

$$Cov\left[\{\lambda\},\{\lambda\}\right] = \sum_{i=1}^{N}\sum_{j=1}^{N}\left.\frac{\partial\{\lambda\}}{\partial\alpha_i}\right|_{\alpha=0}\left(\rho_{ij}\sigma_{\alpha_i}\sigma_{\alpha_j}\right)\left.\frac{\partial\{\lambda\}^T}{\partial\alpha_j}\right|_{\alpha=0} \tag{45}$$

Where

$$\left[\sigma_\alpha\right] = \begin{bmatrix} \sigma_{b1} & \dots & \dots & 0 \\ 0 & \sigma_{b2} & \dots & 0 \\ \dots & \dots & \dots & \dots \\ 0 & \dots & \dots & \sigma_{bm} \end{bmatrix} and \left[\rho_{ij}\right] = \begin{bmatrix} 1 & \rho_{12} & \dots & \rho_{1m} \\ \rho_{21} & 1 & \dots & \rho_{2m} \\ \dots & \dots & .. & \dots \\ \rho_{m1} & \rho_{m2} & \dots & 1 \end{bmatrix} \tag{46}$$

where $[\sigma_\alpha]$, $[\rho_{ij}]$ and m are the standard deviation (SD) of random variables, the correlation coefficient matrix and a number of random variables, respectively. In the present analysis, the uncorrelated Gaussian random variable is taken into consideration. Therefore, covariance is equal to variance.

The variance of the buckling of random variables b_i (i=1, 2,…R) and correlation coefficients can be expressed as

$$\mathrm{var}\{\lambda\} = \left(\frac{\partial\{\lambda\}}{\partial b_i^R}\right)\left[\sigma_\alpha\right]\left[\rho_{ij}\right]\left[\sigma_\alpha\right]\left(\frac{\partial\{\lambda\}}{\partial b_i^R}\right)^T \tag{47}$$

The standard deviation is taken as square root of variance.

The parameters $\left.\frac{\partial\{\lambda\}}{\partial\alpha_i}\right|_{\alpha=0}$ and $\left.\frac{\partial\{\lambda\}}{\partial\alpha_j}\right|_{\alpha=0}$ are the sensitivity of buckling response with respect to random variables.

The second methodology known as Monte Carlo simulation (MCS) is based on the use of random variables and probabilistic statistics by direct use of a computer to investigate the problem. In the problem, a set of random numbers is generated first to represents the statistical uncertainties in the random structural parameters. These random numbers are then substituted into the deterministic response equation to obtain the set of random numbers which reflect the structural response (34, 36). This method is very simple and efficient when used with analytical response functions, but becomes computationally expensive when numerical methods are used to calculate the system response.

Table 1 The effective material properties of CNTRCs Poly methyl methacrylate (PMMA)

Properties of matrix		Properties of reinforcement (CNT)		Efficiency parameter			
Young's modulus	3.52-0.0034T	Young's modulus (E_{12}^{CN})	600 GPa	v_{cn}^{*}	η_1	η_2	η_3
Thermal coefficient (α^m)	$45(1+0.0005\Delta T)\times 10^{-6}/K$	Young's modulus (E_{22}^{CN})	10 GPa	0.12	0.137	1.022	0.715
Density (ρ^m)	1150 Kg/m^3	Shear modulus (G_{12}^{CN})	17.2 GPa	0.17	0.142	1.626	1.138
Poisson's ratio	0.34	Poisson's ration (ν_{12}^{CN})	0.12	0.28	0.141	1.585	1.109

6. Results and discussion

The second-order statistics (mean, COV and PDF) of nonlinear three types of post buckling load of CNTRC elastically supported beam by varying different foundation parameters, support conditions, slenderness ratios, amplitude ratios, and temperature increments, CNTRC distribution (UD, FG-X) with random system properties in MATLAB (R2010a) environment is investigated.

The accuracy of the present probabilistic approach is demonstrated by comparing the results with those available in the literature and by employing MCS.

The basic random variables (b_i) are sequenced and defined as

$$b_1 = \mathrm{E}_{11}^{cn},\, b_2 = V_{cn},\, b_3 = E_m,\, b_4 = V_m,\, b_5 = \upsilon_m, b_6 = E_{22}^{cn},\, b_7 = G_{12}^{cn},\, b_8 = \nu_{cn}, \mathrm{b}_9 = \alpha_m, b_{10} = \alpha_{11}^{cn}, b_{11} = \alpha_{12}^{cn}$$
$$b_{12} = k_1, b_{13} = k_2, b_{14} = k_3$$

where $E_{11}^{cn}, V_{cn}\ E_m, V_m, \nu_m, E_{22}^{cn}, G_{12}^{cn}, \nu_{cn}, \alpha_m, \alpha_{11}^{cn}, \alpha_{12}^{cn}, k_1, k_2$ and k_3 are Young's modulus and volume fraction of carbon nanotube, Young's modulus and volume fraction of the matrix, Poisson's ratios of the matrix, thermal expansion coefficient of carbon nanotube and matrix, and linear Winkler, Shear and nonlinear Winkler foundation parameters, respectively.

In the present analysis, two combinations of displacement boundary conditions are used:

Both edges are simply supported (SS): $u = w = 0$; at $x = 0$, a

Both edges are clamped (CC): $u = w = \theta_x = \psi_x = 0$; at $x = 0$, a

One edge is clamped and other is simply supported (CS):

$$u = w = \theta_x = \psi x = 0;\ \text{at } x = 0 \text{ and } u = w = 0;\ \text{at } x = a$$

The following dimensionless buckling load, foundation parameters and nonlinear to linear buckling ratio are used in the present analysis are:

The dimensionless critical mean post buckling load λ_{cr} is used for mechanical and thermomechanical loading and post buckling temperature λ_{Tcr} is used for thermal loading as,

$$\lambda_o = \lambda_{cr} = \lambda \frac{a^2}{E_o h^3}, \lambda_o = \lambda_{Tcr} = \lambda(\Delta T)_{cr}\,\alpha_m \left(\frac{a}{h}\right)^2, K_1 = k_1 \frac{E_O h^3}{a^4},\ K_2 = k_2 \frac{E_O h^3}{a^2},\ K_3 = k_3 \frac{E_O h}{a^4},$$

$$\lambda_o = \lambda_{cr} = \lambda \frac{a^2}{E_o h^3}, \lambda_o = \lambda_{Tcr} = \lambda(\Delta T)_{cr}\,\alpha_m \left(\frac{a}{h}\right)^2, K_1 = k_1 \frac{E_O h^3}{a^4}, K_2 = k_2 \frac{E_O h^3}{a^2}, K_3 = k_3 \frac{E_O h}{a^4}$$

where λ_{cr} is dimensionless critical mean post buckling load for mechanical and thermomechanical loading, post buckling temperature λ_{Tcr} is used for thermal loading and λ is the dimensional buckling load of CNTRC beam. E_O are the reference value of E^m at room temperature (T_O= 300 K).

Table 2 Convergence studies for thermal, mechanical and thermo-mechanical buckling of CNTRCs beam

No. of element	Type of loading	SS		CC		CS	
		Mean	COV	Mean	COV	Mean	COV
16	Thermal	17.6818	0.1276	58.0268	0.0890	29.8375	0.1105
	Mechanical	4.8181	0.1164	19.2570	0.1027	10.2678	0.1138
	Thermo-Mechanical	3.3276	0.0797	12.6494	0.0730	8.8042	0.0997
20	Thermal	17.8743	0.1274	58.0837	0.0892	29.9134	0.1105
	Mechanical	4.8658	0.1164	19.2049	0.1028	10.2800	0.1138
	Thermo-Mechanical	3.3597	0.0798	12.6152	0.0732	8.8144	0.0997
24	Thermal	18.0855	0.1272	58.1705	0.0893	30.0525	0.1104
	Mechanical	4.9178	0.1164	19.2181	0.1029	10.3207	0.1138
	Thermo-Mechanical	3.3948	0.0798	12.6222	0.0732	8.8485	0.0997
30	Thermal	18.4176	0.1269	58.2466	0.0892	30.2887	0.1102
	Mechanical	4.9993	0.1164	19.2875	0.1029	10.3969	0.1137
	Thermo-Mechanical	3.4498	0.0798	12.6639	0.0733	8.9124	0.0997
40	Thermal	18.9899	0.1264	58.6772	0.0890	30.7305	0.1098
	Mechanical	5.1393	0.1163	19.4537	0.1029	10.5478	0.1137
	Thermo-Mechanical	3.5440	0.0798	12.7650	0.0733	9.0388	0.0997
50	Thermal	19.5745	0.1258	58.9700	0.0887	31.0325	0.1094
	Mechanical	5.2815	0.1163	19.6433	0.1028	10.7085	0.1136
	Thermo-Mechanical	3.6398	0.0799	12.8807	0.0734	9.1734	0.0996
60	Thermal	19.8944	0.1247	59.1687	0.0884	31.6594	0.1090
	Mechanical	5.4249	0.1162	19.8424	0.1028	10.8731	0.1135
	Thermo-Mechanical	3.7362	0.0799	13.0020	0.0734	9.3112	0.0996

A stochastic finite element method (SFEM) based on SOPT and MCS are used to evaluate the expected mean, coefficient of variation (COV) and PDF on the dimensionless post buckling load of CNTRC elastically supported uncertain beam subjected to thermal loading.

The effective material properties of CNTRCs Poly methyl methacrylate (PMMA) is selected for the matrix and the material properties of CNT are temperature dependent by Shen and Xiang (2013) as shown in Table 1.

6.1 Convergence and validation study of second order statistics of post buckling deflection

The convergence study of mean and PDF for thermal, mechanical and thermomechanical post buckling loads by varying number of elements and number of samples are examined by direct iterative procedure combined with SOPT and MCS is shown in Table 2 and Fig. 3. As the number of elements and number of samples increases, the mean value of dimensionless buckling load converses. Therefore, in the present analysis, the total number of elements and samples are taken as 60 and 10, 0000, respectively.

The accuracy and effectiveness of present deterministic FEM results using HSDT for thermal, mechanical and thermomechanical critical post buckling temperature of CNTRC beam supported with and without elastic foundation for UD and FG distribution through various volume fractions

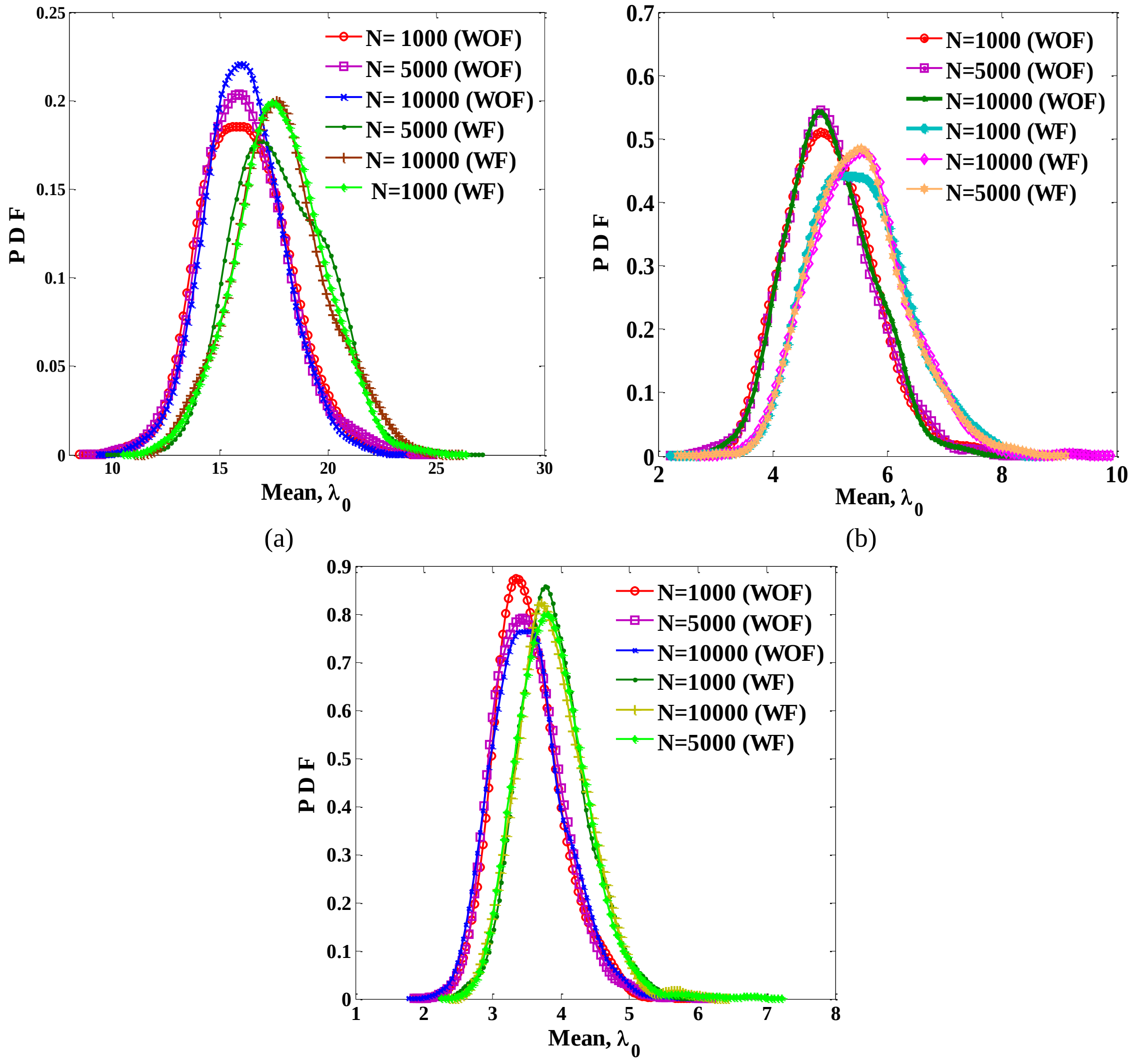

(c)

Fig. 3 The effect of number of samples on the PDF of post buckling load with combined random variables $\{b_i, (i=1 \text{ to } 14)=(0.10)\}$ for (a) thermal buckling (b) mechanical buckling and (c) thermo-mechanical buckling of UD distributed CNTRC beams considering with and without foundation on the following parameters-a/h=25,COC=0.10,V_{cn}=0.17, W_{max}/h=1, $K_1=10^3$, $K_2=10$, $K_3=10^2$, T=300 K

and foundation stiffness are compared with those given by Shen and Xiang (2013) which is based on semi analytical method using HSDT as shown in Figs. 4 and 5. Both accomplished results for given different parameter are in good agreements.

The effect of various mode shapes of thermal, mechanical and thermomechanical post buckling load of UD CNTRC distributed beam is shown in Fig. 6. Among the given post buckling mode shapes of UD CNTRC beam, the first mode buckling load shows the highest amplitude. Therefore, it is concluded that corresponding first buckling load corresponding to the first mode is utmost importance.

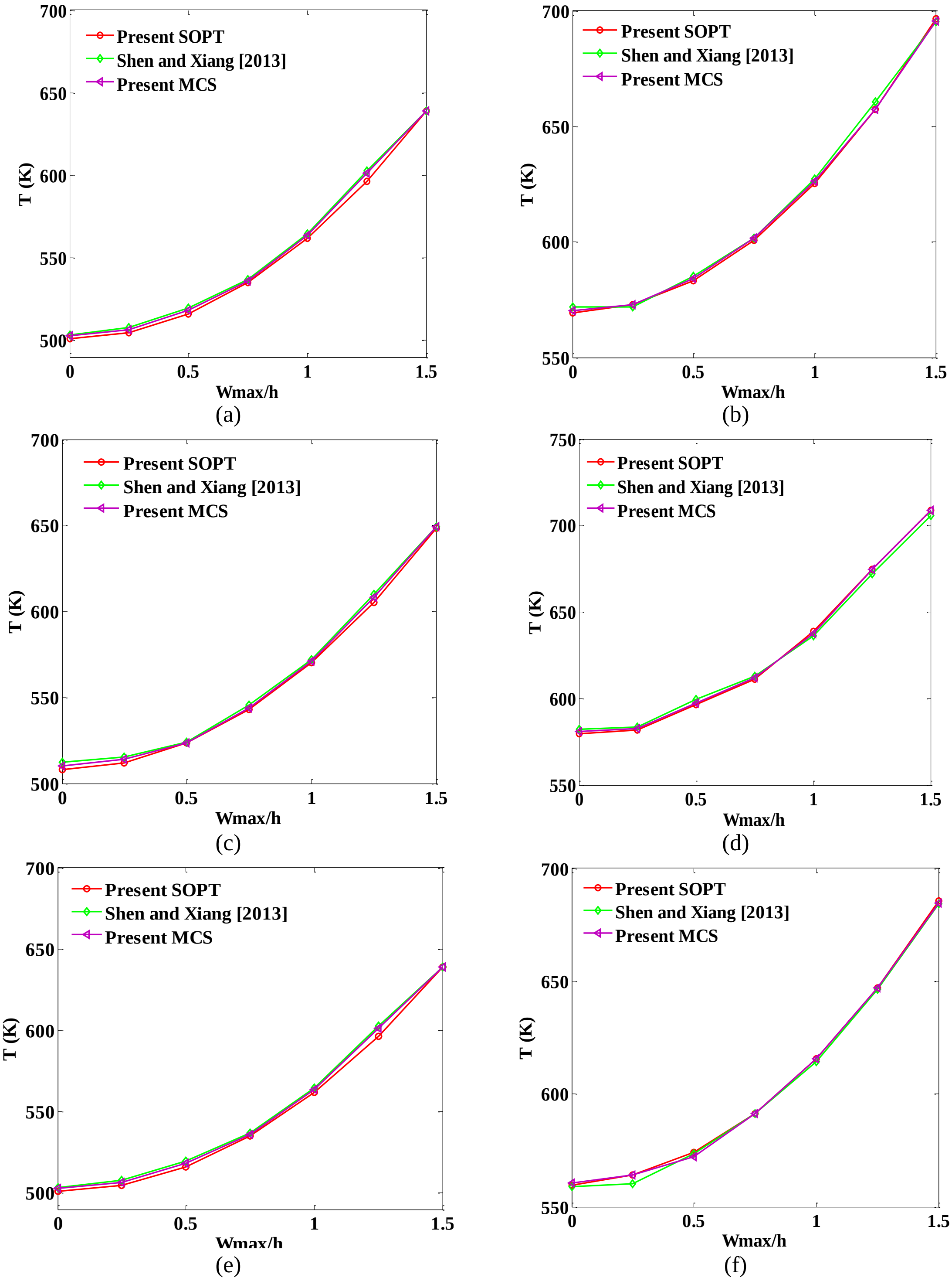

Fig. 4 The effect of volume fraction of CNT for (a) UD and (b) FG-X distribution for V_{cn}=0.12 (c) UD and (d) FG-X distribution for V_{cn}=0.17 (e) UD and (f) FG-X distribution for V_{cn}=0.28 on the critical post buckling temperature of CNTRC beam. (a/h=25)

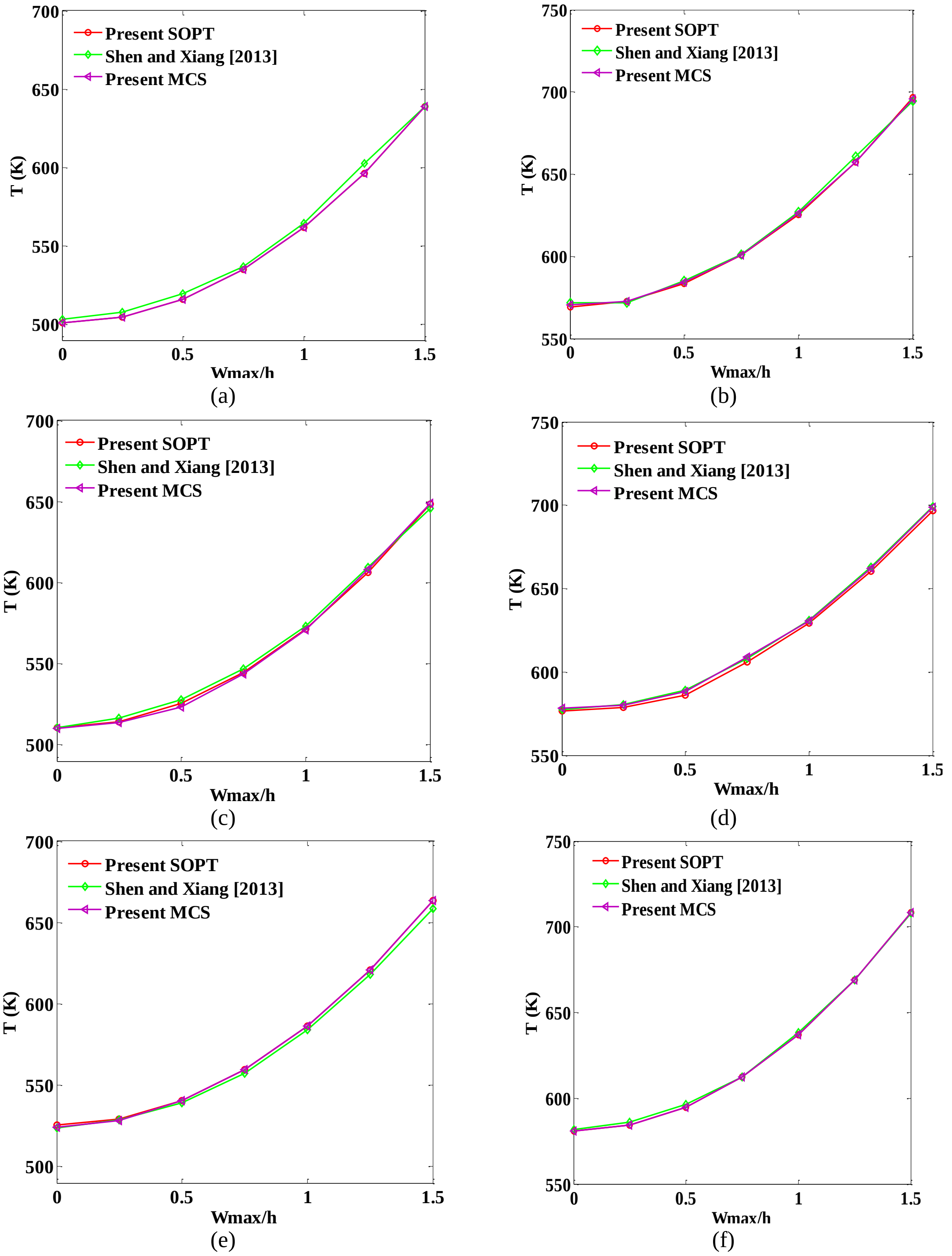

Fig. 5 The effect of the foundation stiffness for (a) UD and (b) FG-X distribution for k_1=0, k_2=0 (c) UD and (d) FG-X distribution for k_1=100, k_2=0 (e) UD and (f) FG-X distribution for k_1=100, k_2=10 on the critical post buckling temperature of CNTRC beam. (V_{cn}=0.12)

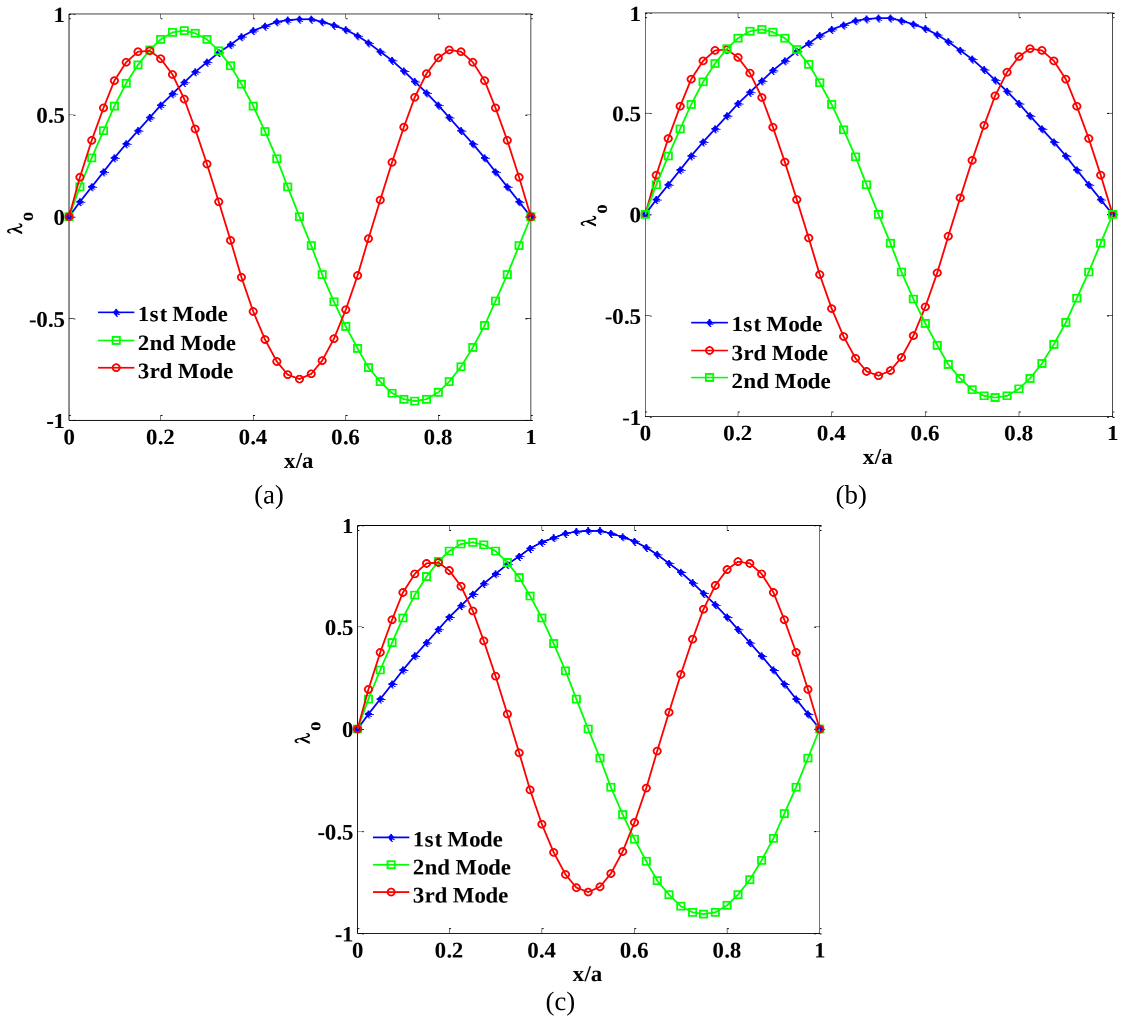

Fig. 6 The effect of mode shape on post buckling load for (a) thermal buckling (b) mechanical buckling and (c) thermo-mechanical buckling load for UD distributed CNTRC beams for a/h=25, V_{cn}=0.17, W_{max}=*1.0*, k_1=0, k_2=0, and k_3=0

6.2 Parametric study of second order statistics of post buckling deflection

Fig. 7 shows the effect of volume fraction on COV and PDF of thermal post buckling load for UD and FG-X distributed CNTRC beams by SOPT and MCS with combined random variables {b_i, (i=1 to 14)=(0.10)} considering with and without foundation. As the volume fraction increases, the mean thermal post buckling load, COV, and dispersion in PDF increases. Considering the effect of the foundation, the thermal post buckling load increases with increase in volume fraction and gives higher values as compared to without foundation.

Fig. 8 shows the effect of slenderness ratio on the COV and PDF of thermal post buckling load for UD and FG-X distributed CNTRC beams by SOPT and MCS with combined random variables {b_i, (i=1 to 14)=(0.10)} considering with and without foundation. As the slenderness ratio

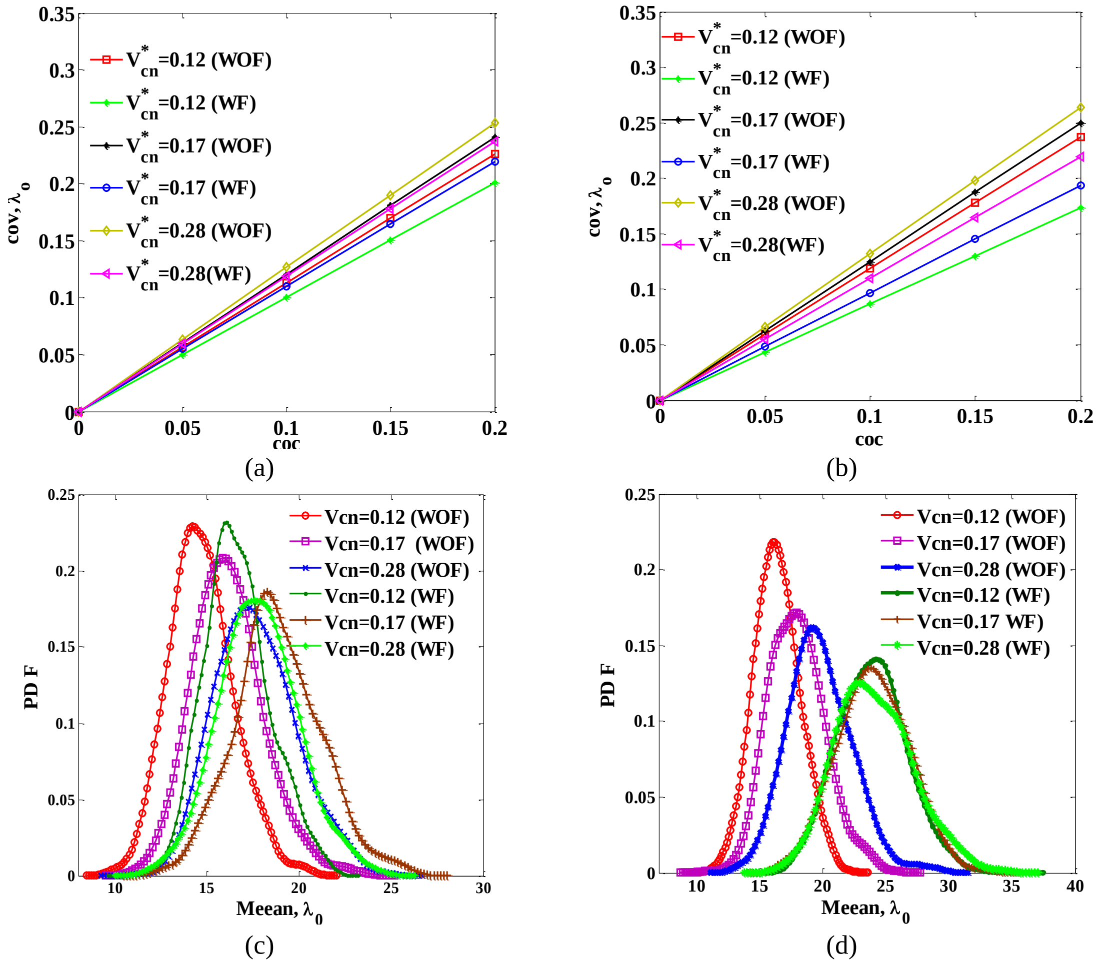

Fig. 7 The effect of volume fraction on COV of thermal post buckling load for (a) UD and (b) FG-X of distributed CNTRC beams and PDF of thermal post buckling load for (c) UD (d) FG-X distributed CNTRC beams with combined random variables {b_i, (i=1 to 14)=(0.10)} considering with and without foundation on the following parameters for a/h=25,COC=0.10, V_{cn}=0.17, W_{max}/h=1, K_1=10^3, K_2=10, K_3=10^2, N=10^4, and T=300 K

increases, the mean thermal post buckling load, COV and dispersion in PDF increases. Considering the effect of the foundation, the thermal post buckling load increases with increase in a/h ratio and gives higher values as compared to without foundation. It is because of foundation parameters increase the stiffness of the beam.

Fig. 9 shows the effect of amplitude ratio on the COV and PDF of thermal post buckling load for UD and FG-X distributed CNTRC beams by SOPT and MCS with combined random variables {b_i, (i=1 to 14)=(0.10)} considering with and without foundation.

As the amplitude ratio increases, the mean thermal post buckling load, COV and dispersion in PDF increases. Considering the effect of the foundation, the thermal post buckling load increases with increase in amplitude ratio and gives higher values as compared to without foundation. It is because of amplitude ratio increase, the beam becomes thinner.

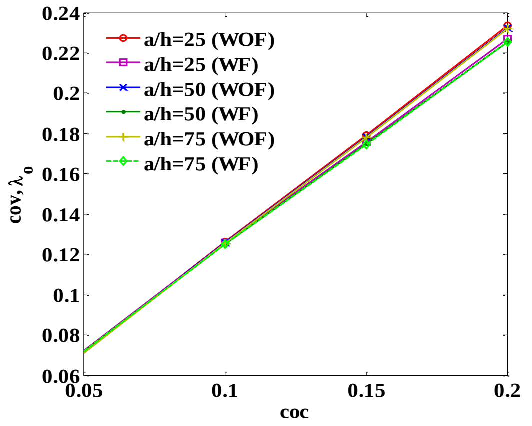

(a)

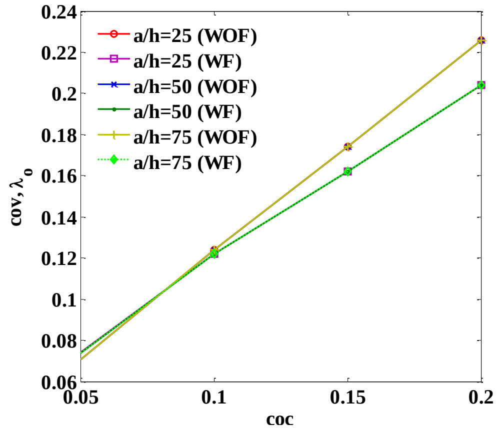

(b)

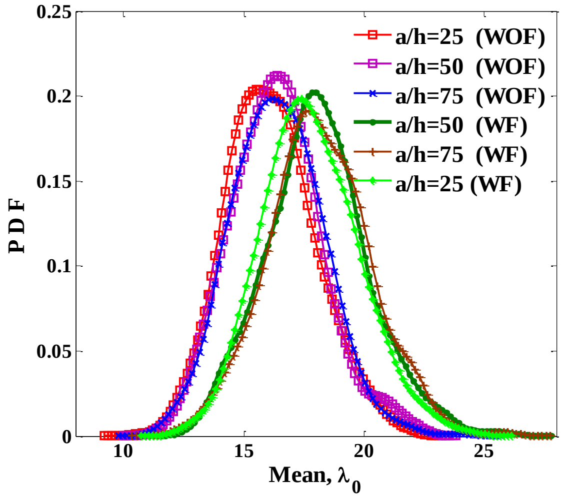

(c)

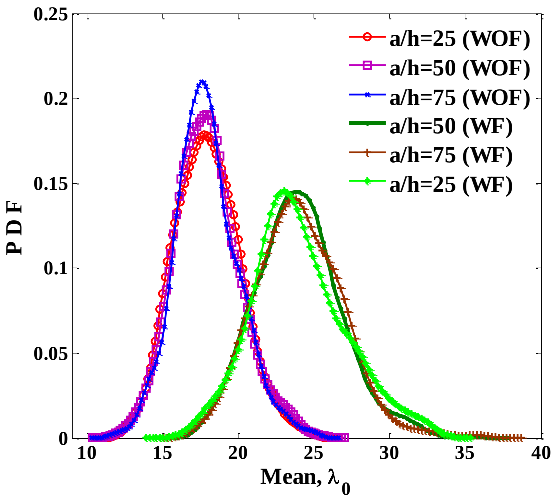

(d)

Fig. 8 The effect of slenderness ratio on COV of thermal post buckling load for (a) UD and (b) FG-X distributed CNTRC beams and PDF of thermal post buckling load for (c) UD (d) FG-X distributed CNTRC beams with combined random variables {b_i, (i =1 to 14) = (0.10)} considering with and without foundation on the following parametersfor a/h=25, COC=0.10, V_{cn}=0.17, W_{max}/h=1, K_1=10^3, K_2=10, K_3=10^2, N=10^4, and T=300 K

Fig. 10 shows the effect of coefficient of covariance (COC) on the PDF of post buckling load with combined random variables {b_i, (i=1 to 14)=(0.05-0.20)} for UD and FG-X by SOPT and MCS in the case of thermal, mechanical and thermomechanical buckling considering with and without foundation of distributed CNTRC beams. As the COC increases from 0.05-0.20, the dispersion in PDF increases by taking effect of all combined random parameters so as tends to more deviate from the mean post buckling load. The dispersion in PDF decreases by taking the effect of foundation for UD and FG-X CNTRC beam in all the case of thermal, mechanical and thermomechanical post buckling load.

Fig. 11 shows the effect of volume fraction on the COV and PDF of post buckling load with combined random variables {b_i, (i=1 to 14)=(0.10)} for UD and FG-X by SOPT and MCS in the

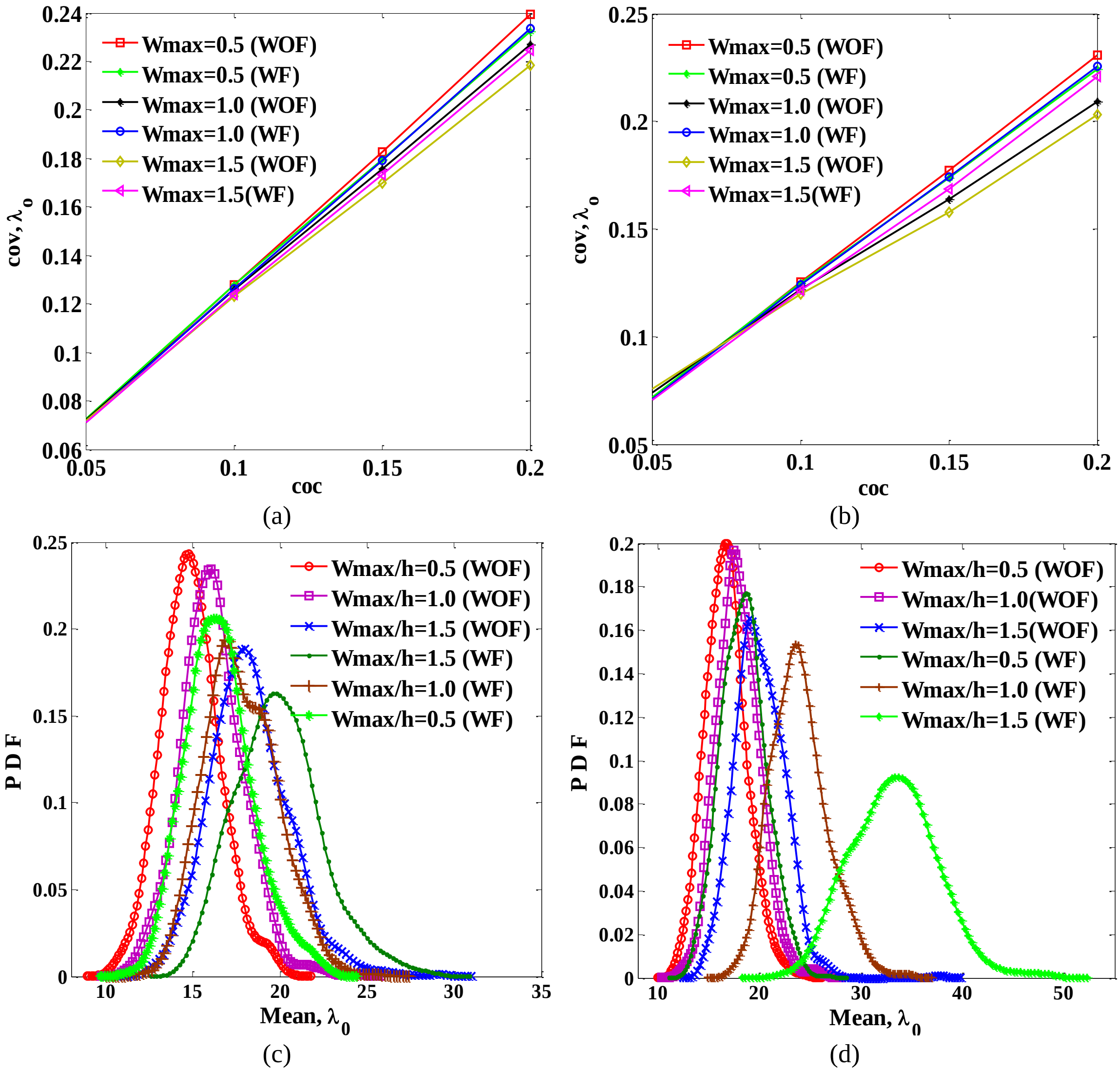

Fig. 9 The effect of amplitude ratio on COV of thermal post buckling load for (a) UD and (b) FG-X and PDF of thermal post buckling load for (c) UD d) FG-X distributed CNTRC beams with combined random variables $\{b_i, (i=1 \text{ to } 14)=(0.10)\}$ considering with and without foundation on the following parameters for $a/h=25$, $COC=0.10$, $V_{cn}=0.17$, $W_{max}/h=1$, $K_1=10^3$, $K_2=10$, $K_3=10^2$, $N=10^4$, and $T=300$ K

case of thermal, mechanical and thermomechanical buckling considering with and without foundation. For the same volume fraction, the COV and dispersion in PDF of thermal post buckling load are higher than mechanical and thermomechanical post buckling load.

Fig. 12 shows the effect of combined random variables $\{b_i, (i=1 \text{ to } 14)=(0.10)\}$ on COV of the postbuckling load with and without foundation for UD and FG-X for thermal of CNTRC distributed beams. As a number of random variables are considered, the COV of thermal post buckling load increases. It is because of the cumulative effect of all random variable on the variance of thermal post buckling load increases.

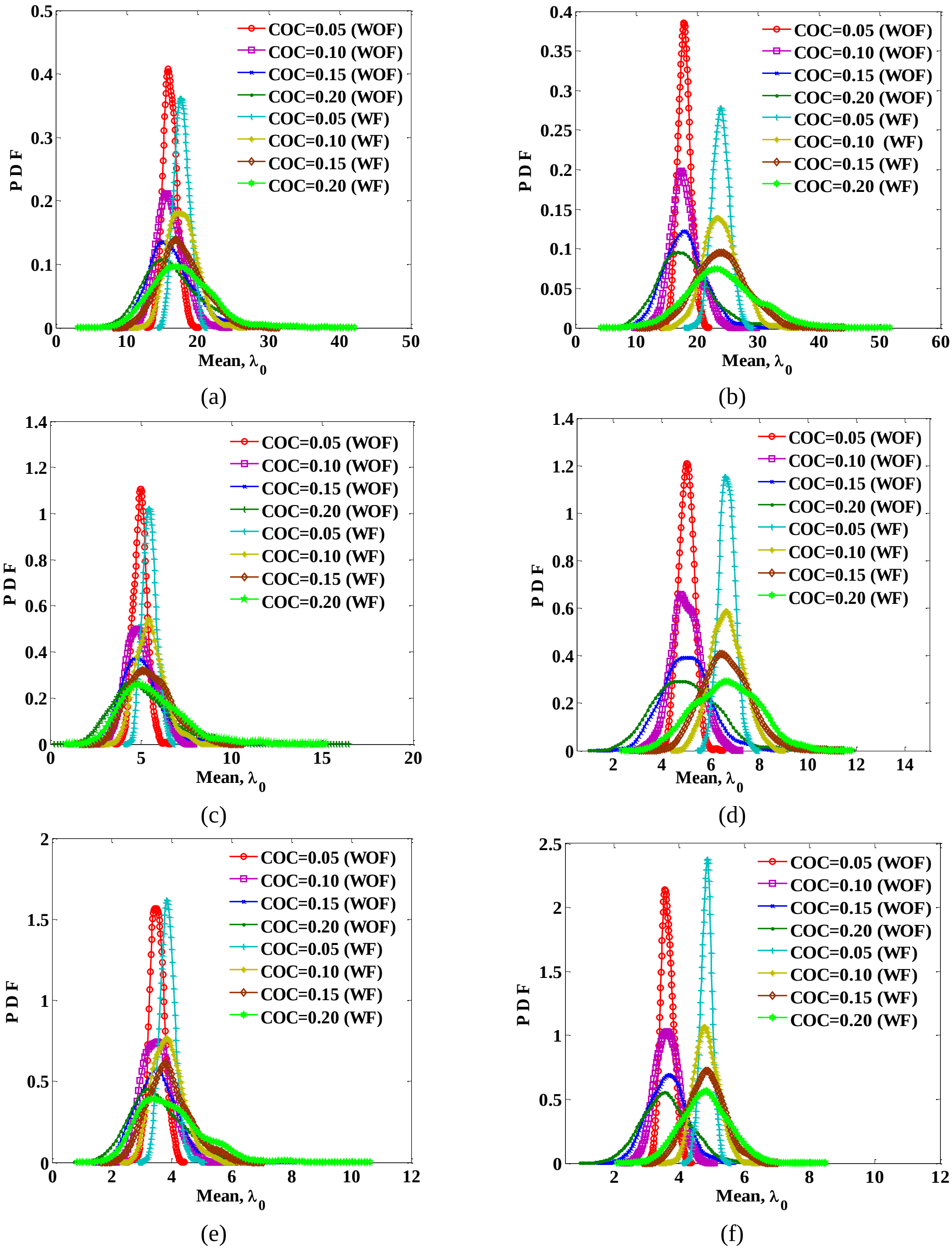

Fig. 10 The effect of COC on PDF of postbuckling load with combined random variables {b_i,(i=1 to 14)=(0.05-0.20)} for thermal buckling of (a) UD and (b) FG-X and for mechanical buckling of (c) UD (d) FG-X and for thermomechanical buckling of (e) UD (f) FG-X distributed CNTRC beams with and without foundation on the following parameters for a/h=25, COC=0.10, V_{cn}=0.17, W_{max}/h=1, K_1=10^3, K_2=10, K_3=10^2, N=10^4, and T=300 K

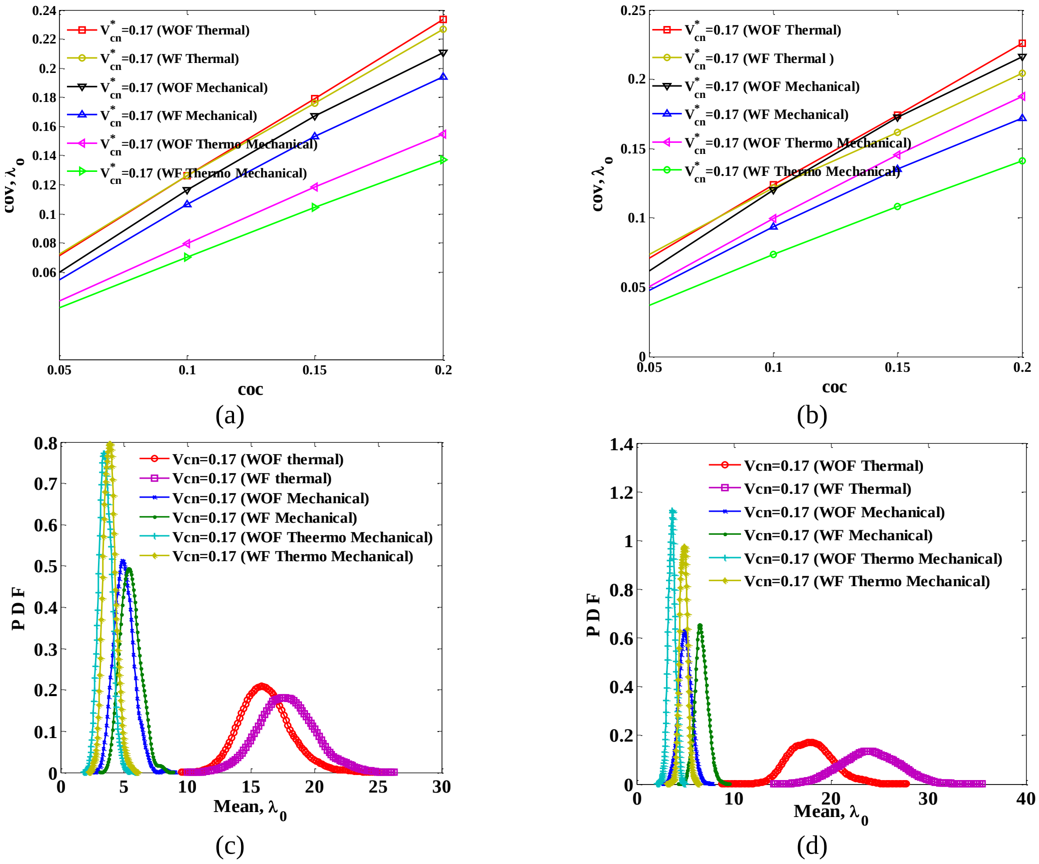

Fig. 11 The effect of volume fraction on COV of post buckling load for (a) UD and (b) FG-X distributed CNTRC beams and PDF of post buckling load for (c) UD (d) FG-X distributed CNTRC beams with combined random variables {b_i, (i=1 to 14)=(0.10)} of thermal, mechanical and thermomechanical buckling considering with and without foundation on the following parameters for a/h=25, COC=0.10, V_{cn}=0.17, W_{max}/h=1, K_1=10^3, K_2=10, K_3=10^2, N=10^4, and T=300 K

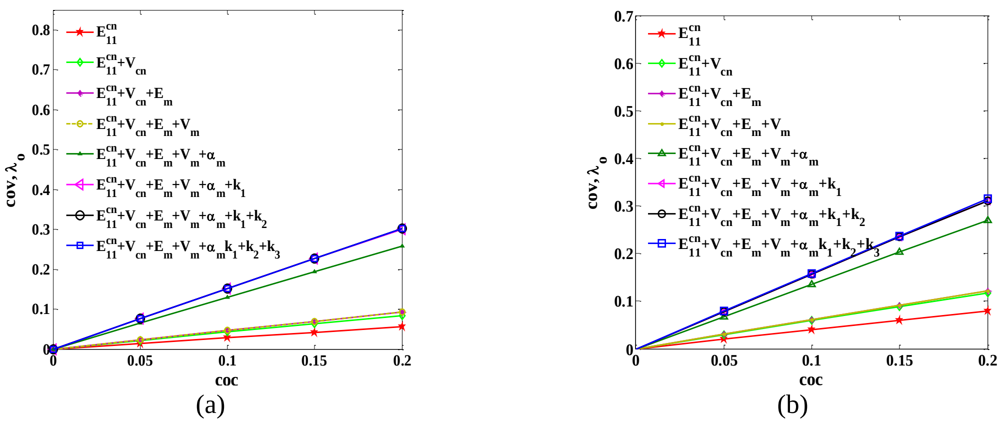

Fig. 12 The effect of combined random variables {b_i, (i=1 to 14)=(0.10)} on COV for UD and (b) FG-X for thermal postbuckling load of CNTRC distributed beams for considering with and without foundation on the following parameters for a/h=25, V_{cn}=0.17, W_{max}/h=1, K_1=10^3, K_2=10, K_3=10^2, and T=300 K

Table 3 Effects of different boundary condition and elastic foundation in case of UD and FG-X for random system properties $\{b_i, (i=1 \text{ to } 11)=0.10\}$ on the mean and COV of thermal, mechanical and thermomechanical post buckling load of CNTRC beam, $a/h=25$, $V_{cn}^* = 0.17, \overline{W}_{\max}/h = 1.0$, $k_1=10^3$, $k_2=10$, $k_2=10^2$

BC	Parameter		Types of loading	FOPT		SOPT		MCS	
				Mean	COV	Mean	COV	Mean	COV
SS	UD	WOF	Thermal	16.1109	0.1489	18.9899	0.1264	16.1240	0.1205
			Mechanical	4.9606	0.1205	5.1393	0.1163	4.9984	0.1291
			Thermomechanical	3.5040	0.0807	3.5440	0.0798	3.5109	0.1059
		WF	Thermal	17.7346	0.1484	19.3524	0.1260	18.6821	0.1083
			Mechanical	5.4605	0.1098	5.6404	0.1063	5.5470	0.1121
			Thermomechanical	3.8571	0.0709	3.8945	0.0702	3.8693	0.0836
	FG-X	WOF	Thermal	17.9476	0.1483	19.4886	0.1238	17.9452	0.1200
			Mechanical	5.0022	0.1250	5.1975	0.1203	5.1327	0.1220
			Thermomechanical	4.2086	0.1018	4.3005	0.0996	4.2586	0.1118
		WF	Thermal	23.8543	0.1480	24.0172	0.1220	23.9696	0.1194
			Mechanical	6.6709	0.0967	6.8787	0.0937	6.6614	0.1008
			Thermomechanical	5.6126	0.0748	5.7008	0.0737	5.5235	0.0732
CC	UD	WOF	Thermal	56.6772	0.1514	58.4998	0.0918	57.6793	0.1160
			Mechanical	17.4510	0.1147	19.4537	0.1029	16.4004	0.1070
			Thermomechanical	12.3270	0.0759	12.7650	0.0733	12.4718	0.0901
		WF	Thermal	57.4685	0.1511	59.5725	0.0913	58.4307	0.1136
			Mechanical	17.6947	0.1128	19.6882	0.1014	16.6687	0.1196
			Thermomechanical	12.4991	0.0743	12.9298	0.0718	12.6435	0.0936
	FG-X	WOF	Thermal	67.3652	0.1483	69.2533	0.0852	67.4984	0.1211
			Mechanical	18.8050	0.1250	20.5660	0.1090	19.2050	0.1280
			Thermomechanical	15.8218	0.1018	17.1195	0.0941	16.8218	0.1038
		WF	Thermal	71.7166	0.1500	73.5421	0.0830	71.9330	0.1167
			Mechanical	20.0400	0.1174	22.8086	0.1032	22.9941	0.1247
			Thermomechanical	16.8608	0.0944	18.1272	0.0878	17.5006	0.0891

Table 3 shows the effects of different support boundary condition and elastic foundation on the mean and COV by FOPT, SOPT and MCS of thermal, mechanical and thermomechanical post buckling load of CNTRC beam supported with (WF) and without (WOF) elastic foundations for UD and FG CNTRC distribution assuming all system properties $\{b_i, (i=1 \text{ to } 14)=0.10\}$ as random variables using SOPT and MCS. For the same boundary condition, the mean post buckling load and COV in the case of UD are lower than FG-X distributed CNTRC beam. As the foundation parameter increases, the mean post buckling load and COV decreases in case of UD and FG-X distributed CNTRC beam for SS and CC support condition.

Table 4 shows the effects of individual random variables (b_i), keeping all others as deterministic in the case of UD and FG with random system properties $\{b_i, (i=1 \text{ to } 14)=0.1\}$ using FOPT, SOPT, and MCS on the mean and COV of thermal post buckling load of CNTRC beam with elastic foundation. Among all the given random system properties, the beam is more sensitive to random

Table 4 Effects of individual random variables (b_i) in the case of UD and FG with random system properties {b_i, (i=1 to 11)=0.1} on the mean and COV of thermal post buckling a load of CNTRC beam with elastic foundation $V^*_{cn} = 0.17$, $\overline{W}_{\max} / h = 1.0$, a/h=25, k_1=10^3, k_2=10, k_2=10^2

RV	Parameter	FOPT		SOPT		MCS	
		Mean	COV	Mean	COV	Mean	COV
b_1= E_{11}^{cn}	UD	17.7346	0.0774	17.8583	0.0735	17.7163	0.0688
	FG-X	23.8543	0.0789	24.4097	0.0739	22.8543	0.0694
b_2=V_{cn}	UD	17.7346	0.0791	17.8920	0.0749	17.7164	0.0719
	FG-X	23.8543	0.0808	24.4097	0.0754	23.8542	0.0788
b_3=E_m	UD	17.7346	0.0286	17.7948	0.0284	17.7381	0.0220
	FG-X	23.8543	0.0257	23.9242	0.0256	23.8655	0.0215
b_4=V_m	UD	17.7346	0.0241	17.7353	0.0237	17.7421	0.0221
	FG-X	23.8543	0.0215	23.8571	0.0212	23.8653	0.0205
b_5=v_m	UD	17.7346	6.7289e-04	17.7346	6.7289e-04	17.7346	1.7073e-04
	FG-X	23.8543	6.7522e-06	23.8543	6.7522e-06	23.8543	4.4899e-06
B_6= G_{12}^{cn}	UD	17.7346	5.3877e-06	17.7346	5.3877e-06	17.7345	5.3877e-06
	FG-X	23.8543	6.9697e-07	23.8543	6.9697e-07	23.8543	1.2208e-06
B_7=α_m	UD	17.7346	0.0160	20.0275	0.0160	17.7051	0.0141
	FG-X	23.8543	0.0174	28.0026	0.0173	23.8159	0.0153
B_8= α_{11}^{cn}	UD	17.7346	0.0834	18.7087	0.0785	17.8470	0.0816
	FG-X	23.8543	0.0821	25.6167	0.0764	24.0110	0.0814
B_9=k_1	UD	17.7346	0.0016	17.7430	0.0016	17.7337	0.0012
	FG-X	23.8543	0.0018	23.8543	0.0018	23.8543	0.0010
B_{10}=k_2	UD	17.7346	0.0678	17.7348	0.0652	17.7346	0.0644
	FG-X	23.8543	0.0605	23.8547	0.0580	23.8543	0.0594
B_{11}=k_3	UD	17.7346	0.0096	17.7346	0.0096	17.7346	0.0087
	FG-X	23.8543	0.0096	24.0148	0.0096	23.8542	0.0097

change in Young's modulus, CNT volume fraction and thermal expansion coefficients, and shear foundation parameters. Tight controls over these random system parameters are required for high reliability of CNTRC elastically supported beam in aerospace and other sensitive applications. The statistics results using MCS are very close to the SOPT results which show the efficacy of present approaches.

7. Conclusions

A probabilistic skill tackled on FOPT and SOPT are established by utilizing the existing deterministic approach to study the second order statistics of thermal, mechanical and thermo-mechanical post-buckling load with von-Karman type nonlinearity of a CNTRC beam in the scaffold of HSDT. The effect of amplitude ratio, thickness ratio, volume fraction, aspect ratio, foundation parameters, various boundary condition and temperature independent and dependent material properties with random change in thermomechanical properties and foundation parameter are examined. The subsequent conclusions are noted from the limited study:

The CNTRC beam is more sensitive to random alteration in Young modulus and volume fraction of CNTRC and shear foundation parameters. For the consistency of the CNTRC elastically supported beam, these parameters should be high accurate measured. FG-X CNTRC distribution shows higher mean and corresponding COV and dispersion in PDF as equated to UD distribution CNTRC beam. The foundation parameters make the mean corresponding COV of buckling load and temperature lowers. In the given thermal, mechanical and thermomechanical loadings, the mean, COV dispersion in PDF for CNTRC elastically supported beam imperiled to mechanical load is highest. As the amplitude ratio increases, the mean, COV, and dispersion in PDF thermal post buckling load and temperature increases. As the slenderness ratio increases, the mean, COV, and dispersion in PDF of post buckling load and temperature increases.

References

Lal, A., Jagtap, K.R. and Singh, B.N. (2013), "Post buckling response of functionally graded material plates subjected to mechanical and thermal loading with random material properties", *Appl. Math. Model.*, **37**(5), 2900-2920.

Lal, A., Singh, N.H. and Shegokar, N.L. (2012), "FEM model for stochastic mechanical and thermal post buckling response of functionally graded material plates applied to panels with circular and square holes having material randomness", *J. Mech. Sci.*, **62**(1), 18-33.

Esawi, A.M.K. and Farag, M.M. (2007), "Carbon nanotube reinforced composites: Potential and current challenges", *Mater. Des.*, **28**(9), 2394-2401.

Singh, B.N. and Grover, N. (2013), "Stochastic methods for the analysis of uncertain composites", *J. Ind. Inst. Sci.*, **93**(4), 603-620.

Salvetat, D. and Rubio, A. (2002), "Mechanical properties of carbon nanotubes: A fiber digests for beginners", *Carbon.*, **40**(10), 1729-1734.

Thostenson, E.T., Ren, Z. and Chou, T.W. (2001), "Advances in the science and technology of carbon nanotubes and their composites: A review", *Compos. Sci. Technol.*, **61**(13), 1899-1912.

Vanmarcke, E. and Grigoriu, M. (1983), "Stochastic finite element analysis of simple beams", *ASCE J. Eng. Mech.*, **109**(5), 1203-1214.

Elishakoffl, Y.J., Ren, M. and Shinozuka. (1996), "Variational principles developed for and applied to analysis of stochastic beams", *ASCE J. Eng. Mech.*, **122**(6), 559-565.

Stefanou, G. (2009), "The stochastic finite element method: past, present and future", *Comput. Meth. Appl. Mech. Eng.*, **15**, 1031-1051.

Seidel, G.D. and Lagoudas, D.C. (2006), "Micromechanical analysis of the effective elastic properties of carbon nanotube reinforced composites", *Mech. Mater.*, **38**(8), 884-907.

Shen, H.S. (1995), "Post buckling analysis of moderately thick rectangular plates on two parameter elastic foundations", *Eng. Struct.*, **17**(7), 523-529.

Shen, H.S. and Zhang, C.L. (2010), "Thermal buckling and post buckling behavior of functionally graded carbon nanotube-reinforced composite plates", *Mater. Des.*, **31**, 3403-3411.

Wan, H., Delale, F. and Shen, L. (2005), "Effect of CNT length and CNT-matrix interphase in carbon nanotube (CNT) reinforced composites", *Mech. Res. Commun.*, **32**(5), 481-489.

Shen, H.S. and Xiang, Y. (2013), "Nonlinear analysis of nanotube-reinforced composite beams resting on elastic foundations in thermal environments", *Eng. Struct.*, **56**, 698-708.

Wuite, J. and Adali, S. (2005), "Deflection and stress behaviour of nanocomposite reinforced beams using a multiscale analysis", *Compos. Struct.*, **71**(3), 388-396.

Yang, J., Liew, K.M. and Kitipornchai, S. (2005), "Stochastic analysis of compositionally graded plates with

system randomness under static loading", *J. Mech. Sci.*, **47**(10), 1519-1541.
Locke, J.E. (1993), "Finite element large deflection random response of thermally buckled plates", *J. Sound Vibr.*, **160**, 301-312.
Rafiee, M., Yang, J. and Kitipornchai, S. (2013), "Thermal bifurcation buckling of piezoelectric carbon nanotube reinforced composite beams", *Comput. Math. Appl.*, **66**(7), 1147-1160.
Yas, M.H. and Samadi, S. (2012), "Free vibrations and buckling analysis of carbon nanotube reinforced composite Timoshenko beams on elastic foundation", *J. Pres. Ves. Pip.*, **98**, 119-128.
Wattanasakulpong, N. and Ungbhakorn, V. (2013), "Analytical solutions for bending, buckling and vibration responses of carbon nanotube-reinforced composite beams resting on elastic foundation", *Compos. Mater. Sci.*, **71**, 201-208.
Dash, P. and Singh, B.N. (2012), "Buckling and post-buckling of laminated composite plates mechanics", *Res. Commun.*, **46**, 1-7.
Bonnet, P., Sireude, D., Garnier, B. and Chauvet, O. (2007), "Thermal properties and percolation in carbon nanotube-polymer composites", *J. Appl. Phys.*, **91**, 2019-2010.
Malekzadeh, P. and Shojaee, M. (2013), "Buckling analysis of quadrilateral laminated plates with carbon nanotubes reinforced composite layers", *Thin-Wall. Struct.*, **71**, 108-118.
Shapery, R.A. (1968), "Thermal expansion coefficients of composite materials based on energy principles", *J. Compos. Mater.*, **2**(3), 380-404.
Reza, H., Hamid, R., Mirdamadi, H. and Khademyzadeh. (2012), "Buckling analysis of short carbon nanotubes based on a novel Timoshenko beam model", *J. Theoret. Appl. Mech.*, **50**(4) 975-986.
Meguid, S.A. and Sun, Y. (2004), "On the tensile and shear strength of nano-reinforced composite interfaces", *Mater. Des.*, **25**(4), 289-296.
Pradhan, S.C. and Reddy, G.K. (2011), "Thermo mechanical buckling analysis of carbon nanotubes on winkler foundation using non-local elasticity theory and DTM", *Ind. Acad. Sci. Sadhana*, **36**(6), 1009-1019.
Hisada, T. and Nakagiri, S. (1980), "A note on stochastic finite element method (part I)-variation of stress and strain caused by shape fluctuation", *J. Inst. Ind. Sci.*, **32**(5), 39-42.
Vodenitcharova, T. and Zhang, L.C. (2006), "Bending and local buckling of a nanocomposite beam reinforced by a single-walled carbon nanotube", *J. Sol. Struct.*, **43**(10), 3006-3024.
Chang, T.P. and Chang, H.C. (1994), "Stochastic dynamic finite element analysis of a non-uniform beam", *J. Sol. Struct.*, **31**(5), 587-597.
Chang, T.P. and Chang, H.C. (1994), "Stochastic dynamic finite element analysis of a non-uniform beam", *J. Sol. Struct.*, **31**(5), 587-597.
Chang, T.P. and Chang, H.C. (1994), "Stochastic dynamic finite element analysis of a non-uniform beam", *J. Sol. Struct.*, **31**(5), 587-597.
Han, Y. and Elliott, J. (2007), "Molecular dynamics simulations of the elastic properties of polymer/carbon nanotube composites", *Comput. Mater. Sci.*, **39**(2), 315-323.
Song, Y.S. and Youn, J.R. (2006), "Modeling of effective elastic properties for polymer based carbon nanotube composites", *Polym.*, **47**(5), 1741-1748.

EC